DOI: https://doi.org/10.57233/ijsgs.v10i3.690 ISSNp: 2488-9229; ISSNe: 3027-1118

IJSGS FUGUSAU VOL. 10 (3) WEBSITE: https://fugus-ijsgs.com.ng

INTERNATIONAL JOURNAL OF SCIENCE FOR GLOBAL SUSTAINABILITY
(A PUBLICATION OF FACULTY OF SCIENCE, FEDERAL UNIVERSITY GUSAU, NIGERIA)

A Farm Land Allocation System using Canny Edge Detection Algorithm (CEDA) and Google Earth

Abubakar Usman Mohammed, Samaila Musa, Lawal Muhammad Jabaka and Garba Muhammad
Department of Computer Science, Federal University Gusau, Nigeria.

Corresponding Author's Email: samailaagp@gmail.com

Received on: August, 2024 **Revised and Accepted on:** September, 2024 **Published on:** October, 2024

ABSTRACT

Farm land allocation in most cases use to be very complex as a result of human error especially when there is paucity of the farm lands. This research focus on the the problem and come with a hybrid solution by combining the Google earth imagery and Canny Edge detection. The Google earth will provide the imagery of the farm lands and the (CEDA) was be used for the allocation and a report will be printed with coordinate of each farm land. The final output of the research helps the three tertiary institutions; Federal University Gusau, Abdu Gusau Polytechnic T/Mafara & College of Agriculture Bakura, Zamfara state in allocating farm land to their staff and communities. Other importance includes: Increase financing income to the institutions, increase Agricultural commodity to the communities, increase capacity utilization of agricultural farms and reduce the level of poverty among the staff/farmers. So also increase efficiency in the records keeping to the institutions.

Keywords: Canny Edga Detection Algorithm, Google Edge, Farmland allocation, staff.

1.0 INTRODUCTION

1.1 Background of the Study

The Canny edge detector is an edge detection operator that uses a multi-stage algorithm to detect a wide range of edges in images and extricate valuable basic data from diverse vision objects and drastically diminish the sum of information to be prepared. It has been broadly connected in different computer vision frameworks (Usman *et al.*, 2024). Canny has found that the prerequisites for the application of edge discovery on differing vision frameworks are generally comparative. Hence, an edge location arrangement to address these prerequisites can be executed in a wide run of circumstances. The common criteria for edge discovery incorporate are detection of edge with low error rate, which means that the detection should accurately catch as many edges shown in the image as possible. The edge point detected from the operator should accurately localize on the center of the edge. A given edge in the image should only be marked once, and where possible, image noise should not create false edges. To fulfill these prerequisites Canny utilized the calculus of varieties – a strategy which finds the work which optimizes a given useful. The ideal work in Canny's finder is depicted by the whole of four exponential terms, but it can be approximated by the primary subsidiary of a Gaussian (Usman *et al.*, 2024). Among the edge location strategies created so distant, Canny edge location algorithm is one of the foremost entirely characterized strategies that gives great and dependable discovery. Owing to its optimality to meet with the three criteria for edge discovery and the effortlessness of process for execution, it got to be one of the foremost well-known calculations for edge discovery (Usman *et al.*, 2024).

One of the first web-based platforms that allowed users to access the large volume of Earth Observation Analysis-Ready-Data (ARD) for rapid large-scale analytics (Gorelick *et al.*, 2017) is Google Earth Engine (GEE), which is currently one of the most comprehensive and powerful platforms for this purpose, with access to more data and analysis. Many studies have used GEE to map ground features ranging from small-scale to large-scale areas, particularly for visualizing, mapping, and modeling purposes (Duan *et al.*, 2020a; Mutanga & Kumar, 2019). The majority of aquaculture extraction studies based on GEE used the spatial and spectral indices using a trial-and-error procedure. This study developed a method for the automated extraction of aquaculture ponds using the Otsu threshold detection model and applied a Canny edge filter to extract the full extent of aquaculture in the Kolleru zone, an important prerequisite for aquaculture management in this area.

Very few studies discussed the drastic changes that occurred in Kolleru Lake as a result of human invasion into aquaculture, which was followed by government restoration efforts that somewhat negatively impacted the environment of the lake (Kolli *et al.*, 2020a). These researchers used remote sensing techniques to examine the fishpond areas up to a contour interval of three feet, based on the land use classification maps. The aquaculture development throughout Kolleru and its tributary Upputeru regions has clearly demonstrated remarkable aquaculture expansion over the years, surpassing its lake area over the past three

DOI: https://doi.org/10.57233/ijsgs.v10i3.690 ISSNp: 2488-9229; ISSNe: 3027-1118

IJSGS FUGUSAU VOL. 10 (3) WEBSITE: https://fugus-ijsgs.com.ng

decades, drawing attention to the international literature due to scalability, massive distribution, and large-scale aquaculture production.

In small-scale farming areas, the application of automatic farmland mapping algorithms utilizing remote sensing data also exhibits subpar performance, according to Du *et al.* (2024). They also proposed a cropland size evaluation index based on edge frequency Excavated Crushed Rock (ECR). To make up for its limits in spatial resolution, the program makes use of the great temporal resolution of Sentinel-2 satellite imagery. Firstly, edge frequencies are computed using all of the Sentinel-2 photos from a given year. This allows the farmland areas to be classified into three categories: high-value permanent edges (PE), medium-value non-permanent edges, and low-value farmed core regions. Subsequently, the edge frequencies undergo two iterative applications of Otsu's thresholding technique, with the goal of extracting edges initially, and then permanently.

Next, the PE to cropland ratio (ECR) is computed. The proper estimation radius for ECR was found to be 1600 m by using the North China Plain and Northeast China Plain as research locations and comparing with current agricultural size records. According to the study, the North China Plain's peak ECR value was 0.105, whereas the Northeast China Plain's top value was 0.085. Overall, the distribution agreed with the dataset used as a reference. According to Cheng *et al.* (2020) and Zhang *et al.* (2020), there are two types of automatic agricultural size mapping techniques that use remote sensing images: edge-based and region-based.

The third strategy is survey-based methods, which are different from crowdsourcing and automatic agricultural size mapping techniques but have very coarse temporal and spatial resolution in the statistical data (Lowder *et al.*, 2021). Systematic censuses are usually only carried out once every few years due to expensive expenses, and data released at the lowest administrative unit cannot accurately portray regional variances. Additionally, there are notable disparities in the estimates of worldwide smallholder farming among scholars due to variances in statistical quality, such as whether or not cultivated land includes permanent grassland or whether the size relates to farm size or farmland size. 84% of the 608 million farms worldwide operate on less than 2 hectares of land, according to a study published in the journal World Development (Lowder *et al.*, 2021). They produce around 35% of the world's food and occupy 12% of the global agricultural area. Approximately half of all tiny farms worldwide are operated by 98% of farmers in China, where the average farm size is less than 2 hectares. Smallholder farming methods are out of step with the advancements in modern agriculture. For instance, dispersed smallholders have difficulty building up the money required for modern agriculture, and fragmented farmland makes it impossible to employ heavy agricultural machines. In order to solve this, the Chinese government promotes land consolidation and transfer, grouping small plots together into bigger ones and putting farmland under the control of a small number of farmers in order to support large-scale farming operations (Rogers *et al.*, 2021). The Chinese government is actively promoting this concentration of cropland, and it is happening quite quickly. But there is a deficiency of suitable methods to track this process timely, accurately, and cost-effectively.

Regular and extensive monitoring must take into account the generalization ability of algorithms and data costs (Xu *et al.*, 2023; Xiao *et al.*, 2021). The amount of the world's farmland can be estimated visually by crowdsourcing, despite the fact that earth observation equipment is extremely sophisticated and can view the surface at a sub-meter level. However, because of the enormous labor costs involved, this method cannot be used as a regular monitoring technique. According to Cheng *et al.* (2020) and Wang *et al.* (2023), automated farmland border detection algorithms are not yet developed sufficiently for use in small farming areas and are unable to balance cost and efficiency. Regarding techniques, while there are numerous object-oriented classification algorithms available, such as those found in Trimble eCognition software version 9, deep learning models are represented by the Segment Anything Model (SAM) (Kirillov, *et al.*, 2023), there are certain restrictions on these algorithms. As per Xu *et al.* (2023), there are numerous parameters in the multi-resolution segmentation method of eCognition software v.9 that need to be altered. Additionally, Wang *et al.* (2023) have mentioned that deep learning models necessitate a substantial amount of training data and extremely high computing costs.

A computer application called Google Earth creates a three-dimensional depiction of the planet mostly using satellite imagery. The application allows users to view cities and landscapes from different perspectives by mapping the Earth by superimposing satellite photos, aerial photography, and GIS data onto a three-dimensional globe. With its desktop application, Google Earth offers numerous additional tools, one of which is a tool for measuring distance. There are extra globes for the Moon and Mars in addition to a night sky viewing instrument. There's also a game for a flying simulator. Users can see uploaded photos from different locations with additional capabilities. Federal University Gusau, Abdu Gusau Polytechnic T/Mafara & College of Agriculture Bakura, Zamfara state have farmland that are being shared to staff for cultivation however the sharing is done by some selected staff

DOI: https://doi.org/10.57233/ijsgs.v10i3.690 ISSNp: 2488-9229; ISSNe: 3027-1118

which lead to human error in the allocation among which include:
Unequal allocation: ideally the allocation supposed to be equal but the measurement tends to have problem, where an individual that paid for a hectare may either be allocated with more or less than a hectare where the accuracy in the allocation is compromise. Structure in a given farmland: this is also another problem because an individual will be given a hectare with a structure which may consume certain percentage of the land and it will be term as a hectare. These are serious problems that require technological approach. The objectives of the research include: Increase financing income to the institutions. Increase Agricultural commodity to the communities. Increase capacity utilization of agricultural farms. Reduce the level of poverty among the staff/farmers. Increase efficiency in the records keeping to the institutions.

Pixel intensity discontinuities describe the boundaries between items in a picture. An operator (a 2-D filter) developed to be sensitive to big gradients in the picture while returning values of zero in uniform areas is almost universally used for edge detection. The number of edge detection operators is staggering, and each one is optimized for detecting certain kinds of edges. Edge orientation, noise environment, and edge structure are all factors to consider when selecting an edge detection operator. The discontinuity in gray level values is what gives an edge its distinctive appearance. This means that an edge denotes the point at which one item ends and another begins. Many factors influence the appearance of picture edges, including: A digital image's luminance fluctuates suddenly at some spots, and the object's geometric and optical features, as well as mathematical algorithms for edge recognition are used to identify these points (or put differently, has discontinuities). The objectives of the research include: increase financing income to the institutions, increase Agricultural commodity to the communities, increase capacity utilization of agricultural farms, reduce the level of poverty among the staff/farmers and increase efficiency in the records keeping to the institutions.

2.0 RESEARCH METHODOLOGY

The implementation works based on the framework presented for Farm Land Allocation using Canny Edge Detection Algorithm and Google Earth algorithms (Usman *et al.*, 2024). The model is based on three algorithms, Algorithms 1, 2, and 3. The Google earth will provide the imagery of the farm lands and the Canny edge detection algorithm will be used for the allocation and a report will be printed with coordinate of each farm land.

2.1 Algorithms 1

Algorithm 1 uses image and generate the edges of the image by using parameters where parameters of edge detecting filters: X-axis direction filter: Y-axis directions filter. The thresholding parameter *alfa*. It will get the initial land image from Google earth and use X-axis direction edge detection, Y-axis direction edge detection Norm of the gradient (Combining the X and Y directional derivatives) Thinning (Using interpolation to find the pixels where the norms of gradient are local maximum.)

Algorithm 1

```
Begin
  Nx1←10;Sigmax1←1;Nx2←10;Sigmax2←1;Theta1←pi/2;
  Ny1←10;Sigmay1←1;Ny2←10;Sigmay2←1;Theta2←0;
  alfa←0.1;
   Land_image←('https://earth.google.com/web/search/federal+university+gusau/@12.13182601,6.79286692,469.2053278a,94.4237725d,35y,-
   100.39885593h,70.72988377t,0r/data =CigiJgokCW3yLZEHQy hAEUvtq KCLPChAGcAfxLHtIBtAIZK0zSfmFRtA');      [x,map] ←
   gifread(Land_image) ;
   w←ind2gray(x,map);
   figure(1);colormap(gray);
   subplot(3,2,1);
   imagesc(w,200);
   subplot(3,2,2);
   filterx←Call(d2dgauss(Nx1,Sigmax1,Nx2,Sigmax2,Theta1));
   Ix← conv2(w,filterx,'same');
   imagesc(Ix);
   title('Ix');
  subplot(3,2,3)
  filtery←Calld2dgauss(Ny1,Sigmay1,Ny2,Sigmay2,Theta2);
  Iy←conv2(w,filtery,'same');
  imagesc(Iy);
   title('Iy');
   subplot(3,2,4);
   NVI←sqrt(Ix.*Ix+Iy.*Iy);
   imagesc(NVI);
   title('Norm of Gradient');
   I_max←max(max(NVI));
   I_min←min(min(NVI));
   level←alfa*(I_max-I_min)+I_min;
   subplot(3,2,5);
   Ibw←max(NVI,level.*ones(size(NVI)));
   imagesc(Ibw);
   title('After Thresholding');
   subplot(3,2,6);
   [n,m] ←size(Ibw);
for i←2:n-1,
    for j←2:m-1,
            if Ibw(i,j) > level,
                    X← [-1,0,+1;-1,0,+1;-1,0,+1];
                    Y← [-1,-1,-1;0,0,0;+1,+1,+1];
                    Z← [Ibw(i-1,j-1),Ibw(i-1,j),Ibw(i-1,j+1);
                    Ibw(i,j-1),Ibw(i,j),Ibw(i,j+1);
                    Ibw(i+1,j-1),Ibw(i+1,j),Ibw(i+1,j+1)];
                    XI← [Ix(i,j)/NVI(i,j), -Ix(i,j)/NVI(i,j)];
```

DOI: https://doi.org/10.57233/ijsgs.v10i3.690 ISSNp: 2488-9229; ISSNe: 3027-1118

IJSGS FUGUSAU VOL. 10 (3) WEBSITE: https://fugus-ijsgs.com.ng

2.2 Algorithm 2

Function "d2dgauss.m": This function returns a 2D edge detector (first order derivative of 2D Gaussian function) with size n1*n2; theta is the angle that the detector rotated counter clockwise; and sigma1 and sigma2 are the standard deviation of the gaussian functions. Function "dgauss.m"(first order derivative of gauss function).

Algorithm 2

```
Begin
function h ← d2dgauss(n1,sigma1,n2,sigma2,theta)
r← [cos(theta) -sin(theta); sin(theta)  cos(theta)];
for i ←1 : n2
            for j ← 1 : n1
                    u ← r * [j-(n1+1)/2 i-(n2+1)/2]';
                     h(i,j) = Call(gauss(u(1),sigma1)*dgauss(u(2),sigma2));
            end
end
h ← h / sqrt(sum(sum(abs(h).*abs(h))));

function y ← Call(gauss(x,std))
y ←exp(-x^2/(2*std^2)) / (std*sqrt(2*pi));

function y =Call dgauss(x,std)
y  ← -x * gauss(x,std) / std^2;
end
```

2.3 Algorithm 3

Function " getMapCoordsByLatAndLng": This function returns longitude and latitude of the mapWidth and mapHeight using (longitude + 180)* (mapWidth / 360 and (mapHeight / 2) - (mapWidth *mercN/(2 * Math.PI)).

Algorithm 3

```
Begin
  function getMapCoordsByLatAndLng(latitude, longitude, mapWidth, mapHeight){
    x ← (longitude + 180 )* (mapWidth / 360);
    latRad ← latitude* Math.PI /180;
    mercN←Math.log(Math.tan(( Math.PI /4)+(latRad/2)));
    y← (mapHeight / 2) - ( mapWidth *mercN/(2 * Math.PI));
    return {
      x: x,
      y: y
    };
   }
  function getMapCoords(latitude, longitude, mapWidth, mapHeight){
     return {
        x: parseInt((longitude + 180.0) * (mapWidth / 360.0)),
        y: parseInt(((latitude * -1.0) + 90.0) * (mapHeight / 180.0))
     }
  }
End
```

DOI: https://doi.org/10.57233/ijsgs.v10i3.690 ISSNp: 2488-9229; ISSNe: 3027-1118

IJSGS FUGUSAU VOL. 10 (3) WEBSITE: https://fugus-ijsgs.com.ng

3.0 RESULTS

The results of implementing Algorithms 1, 2, and 3 are shown in Figures 1, 2, and 3. Figure 1 shows the land image captured from Google Earth. Figure 2 presented the land image from Google and the edges detected from the image and Figure 3 presented the result indicating the coordinate point allocated to each staff by their Senior Personnel (SP) and Junior Personnel (JP) numbers, both the longitudes and the latitudes.

Figure 1: Land image captured from Google Earth.

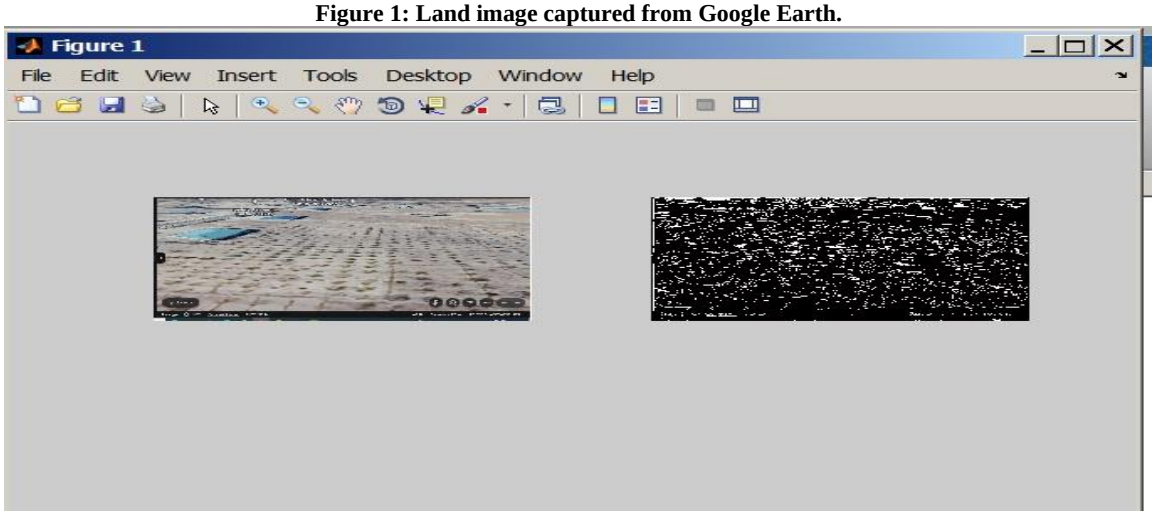

Figure 2 : Land Image From Google

Figure 3 shows the result indicating the coordinate point allocated to each staff by their SP numbers, both the longitude and the latitude. Staff with SP number Sp00xxx1 is allocated land with longitude 12.0704 and latitude 6.0712. Staffs with SP. numbers Sp00xxx4 and Sp00xxx9 are located land with the same longitude but different latitude of 6.0709 and 6.0704 respectively. Staffs with SP. numbers Sp00xxx5 and Sp00xxx7 are located land with the same longitude of 12.0712, but different latitude of 6.0708 and 6.0702 respectively. Staff with SP. numbers Sp00xxx2 and Sp00xxx3 are located land with longitudes of 12.0706 and 12.0708, and latitudes of 6.0711 and 6.071 respectively. So also staff with SP. numbers Sp00xxx6 and Sp00xxx8 are located on land with the longitudes of 12.0714 and 12.0718, and different latitudes of 6.0708 and 6.0706 respectively.

DOI: https://doi.org/10.57233/ijsgs.v10i3.690 ISSNp: 2488-9229; ISSNe: 3027-1118

IJSGS FUGUSAU VOL. 10 (3) WEBSITE: https://fugus-ijsgs.com.ng

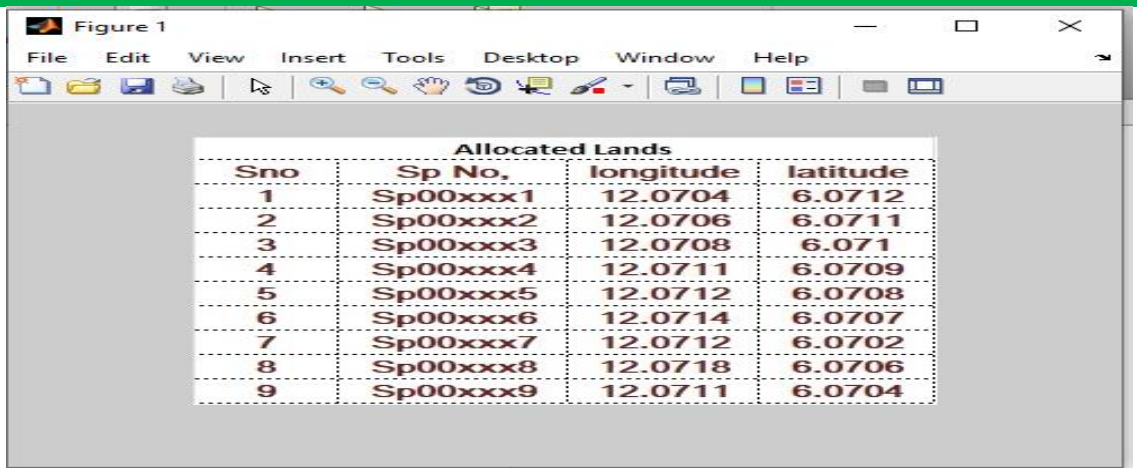

Allocated Lands

Sno	Sp No.	longitude	latitude
1	Sp00xxx1	12.0704	6.0712
2	Sp00xxx2	12.0706	6.0711
3	Sp00xxx3	12.0708	6.071
4	Sp00xxx4	12.0711	6.0709
5	Sp00xxx5	12.0712	6.0708
6	Sp00xxx6	12.0714	6.0707
7	Sp00xxx7	12.0712	6.0702
8	Sp00xxx8	12.0718	6.0706
9	Sp00xxx9	12.0711	6.0704

Figure 3 : The Coordinate Point Allocated to each Staff by their SP Number.

4.0 DISCUSSION

Many studies have been conducted to extract aquaculture ponds using remote sensing satellite images. As a result of the signal's ability to penetrate through the canopy, detect standing water beneath vegetation, and better identify spectral and textural characteristics of an image, the most significant approach using Sentinel-1 images is fully automated, has a high spatial resolution, and a longer wavelength that can distinguish the properties under the vegetation. However, SAR-VV polarization is ideal for the study of aquaculture ponds. Our study performed the automatic extraction method on SAR images for aquaculture mapping in the Kolleru zone. The Otsu method of determining the optimal threshold for detecting the aquaculture pixels based on the Canny edge operator achieved high accuracy. This method can be adopted for dense inland aquaculture mapping in large 10 areas. Several studies focused on extracting massive distribution of aquaculture ponds from adjacent rivers, lakes, and wetlands.

It is challenging to divide individual aquaculture ponds without removing the dikes that separate them. Duan *et al.* (2020a) created a technique to extract ponds by integrating spectral, spatial, and morphological data and believed that the aquaculture region was generally compatible with aquaculture land use parameters. However, the efficacy of these research is constrained if it has to do with small ponds that have been combined or left out. Aquaculture ponds can be segmented or extracted by the use of pertinent indices such as water index, texture, and geometric metrics obtained from radar backscatter. This process greatly enhances the classification outcomes (Sun *et al.*, 2020). However, Wang *et al.* (2020) suggested a technique based on phenology and pixels to map coastal wetlands on a broad scale. The study's very high accuracy of 98% was attained utilizing the pixel-based approach, as the data showed. Another technique for mapping flooded areas is image segmentation, which employs object-based features (OBF) to discern between ponds used for aquaculture and those not (Yu *et al.*, 2020).

The roads and dikes divide the aquaculture pond area, which is a body of stagnant water. With other spectral patterns present, it is challenging to discern the ponds' backdrop using threshold and water index. To improve pond conditions, current research has developed an automated extraction technique for aquaculture ponds that makes use of threshold selection, machine learning models, and object-based approaches mapping accuracy (Duan *et al.*, 2020b). The threshold selection is a set of pixels with a similar value that adapts to extract ponds. For instance, Xia *et al.* (2020) showed that the multi-threshold connected 384 component segmentation and random forest classification model could be used to automatically extract 383 aquaculture ponds. This approach is highly suggested for the non-intensive aquaculture ponds, and they were able to achieve an overall accuracy of 91.8%. The research was centered on the edge detection operator for automatically extracting aquaculture ponds using the Canny Edge Otsu threshold method. The primary goal was to extract the massive aquaculture ponds while also precisely delineate the small size ponds.

When Google launched the Google Earth Engine (GEE) in 2010 to improve the use of satellite imagery for large-scale and time series applications, it was one of the first companies to facilitate the transition towards adopting EO big data cloud platforms. Every data source on GEE has a unique time series of EO/ARD data arranged into an Image Collection stack. Earth observation data integration into GEE systems for possible applications in precision

agricultural analysis for economic development policies, monitoring of land, and spotting changes in the world's forests. This framework can be used to extract information for aquaculture monitoring using GEE.

Figure 3 shows the result indicating the coordinate point allocated to each staff by their SP numbers, both the longitude and the latitude. Staff with SP. number Sp00xxx1 is allocated land with longitude 12.0704 and latitude 6.0712. Staffs with SP. numbers Sp00xxx4 and Sp00xxx9 are located land with the same longitude that shows different farm land can be on the longitude, but different latitude as staff with SP. number Sp00xxx4 in on latitude of 6.0709 while staff with SP. Number Sp00xxx9 in on latitude of 6.0704. Staffs with SP. numbers Sp00xxx5 and Sp00xxx7 are located on land with the same longitude of 12.0712, but also on different latitude of 6.0708 and 6.0702 respectively. Staffs with SP. numbers Sp00xxx2 and Sp00xxx3 are located land with different longitudes of 12.0706 and 12.0708, and also on different latitudes of 6.0711 and 6.071 respectively. So also staffs with SP. numbers Sp00xxx6 and Sp00xxx8 are located on land with the longitudes of 12.0714 and 12.0718, and different latitudes of 6.0708 and 6.0706 respectively.
Farmland plot monitoring is a crucial part of worldwide digital agricultural techniques. In order to extract farmland parcels from high-resolution remote sensing photos, this study suggests a novel methodology. The study's primary findings indicate that our suggested model can be applied to the extraction of high-performing cropland field plots, particularly in regions with severe and intricate fragmentations.

.

5.0 CONCLUSION

In this study, we outlined the shortcomings of previous studies; recognize the importance of spatially local topological information, local repair and enhanced Gaussian-based optimization strategies. We propose a multi-task cascade network model for cropland parcel extraction. This multitask model can automatically learn multi-scale and multi-level features and perform the overall learning through a specially designed network for complex cropping scenarios and multi-scale cropland parcels.

To assess the robustness of the model, experiments were conducted in the study areas of tertiary institutions in Zamfara state; Federal University Gusau, Abdu Gusau Polytechnic T/Mafara & College of Agriculture Bakura, Zamfara state. The results show that this model can extract accurate information about cropland parcels and achieve better consistency with the satellite datasets in terms of spatio-temporal characteristics. Our proposed model is expected to be integrated with practical agricultural observation systems, and thus to contribute to the development of a global agricultural information management platform.

REFERENCES

Cheng, T.; Ji, X.; Yang, G.; Zheng, H.; Ma, J.; Yao, X.; Zhu, Y.; Cao, W. DESTIN: A new method for delineating the boundaries of crop fields by fusing spatial and temporal information from WorldView and Planet satellite imagery. *Comput. Electron. Agric.* **2020**, *178*, 105787.

Du, J., Xu, S., Li, J., Duan, J., & Xiao, W. (2024). A Novel Approach for Farmland Size Estimation in Small-Scale Agriculture Using Edge Counting and Remote Sensing. *Remote Sensing*, *16*(16), 2981.

Duan, Y.; Li, X.; Zhang, L.; Chen, D.; Liu, S.; Ji, H. (2020a). Mapping national-scale aquaculture ponds based on the Google Earth Engine in the Chinese coastal zone. Aquaculture, 520, 734666.

Duan, Y.; Li, X.; Zhang, L.; Liu, W.; Liu, S.; Chen, D.; Ji, H. (2020b). Detecting spatiotemporal changes of large-scale aquaculture ponds regions over 1988-2018 in Jiangsu Province, China using Google Earth Engine. Ocean & Coastal Management, 188, 105144.

Gorelick, N.; Hancher, M.; Dixon, M.; Ilyushchenko, S.; Thau, D.; Moore, R. (2017). Google Earth Engine: Planetary-scale geospatial analysis for everyone. Remote Sensing of Environment, 202, pp: 18-27.

Kirillov, A.; Mintun, E.; Ravi, N.; Mao, H.; Rolland, C.; Gustafson, L.; Xiao, T.; Whitehead, S.; Berg, A.C.; Lo, W.-Y.; *et al.* Segment Anything. 2023. Available online: **http://arxiv.org/pdf/2304.02643** (accessed on 15 August 2024).

Kolli, M.K.; Opp, C.; Karthe, D.; Groll, M. (2020a). Mapping of Major Land-Use Changes in the Kolleru Lake Freshwater Ecosystem by Using Landsat Satellite Images in Google Earth Engine. Water 2020, 12, 2493. https://doi.org/10.3390/w12092493.

Lowder, S.K.; Sánchez, M.V.; Bertini, R. Which farms feed the world and has farmland become more concentrated? *World Dev.* **2021**, *142*, 105455.

Mutanga, O.; Kumar, L. (2019). Google Earth Engine Applications. Remote Sensing, 11(5), 591.

Rogers, S.; Wilmsen, B.; Han, X.; Wang, Z.J.-H.; Duan, Y.; He, J.; Li, J.; Lin, W.; Wong, C. Scaling up agriculture? The dynamics of land transfer in inland China. *World Dev.* **2021**, *146*, 105563.

Sun, Z.;Luo, J.; Yang, J.; Yu, Q.; Zhang, L.; Xue, K.; Lu, L. (2020). National-scale mapping of coastal aquaculture ponds with Sentinel-1 SAR data using Google Earth Engine, Remote Sens, 12, 3086. https://doi.org/10.3390/rs12183086.

Wang, S.; Zhou, Y.; Yang, X.; Feng, L.; Wu, T.; Luo, J. BSNet: Boundary-semantic-fusion network for farmland parcel mapping in high-resolution satellite

images. *Comput. Electron. Agric.* **2023**, *206*, 107683.

Xia, Z.; Guo, X.; Chen, R. (2020). Automatic extraction of aquaculture ponds based on Google Earth Engine. Ocean and Coastal Management, 198, 105348. https://doi.org/10.1016/j.ocecoaman.2020.105348.

Xiao, W.; Xu, S.; He, T. Mapping Paddy Rice with Sentinel-1/2 and Phenology-, Object-Based Algorithm—A Implementation in Hangjiahu Plain in China Using GEE Platform. *Remote Sens.* **2021**, *13*, 990.

Xu, S.; Xiao, W.; Ruan, L.; Chen, W.; Du, J. Assessment of ensemble learning for object-based land cover mapping using multi-temporal Sentinel-1/2 images. *Geocarto Int.* **2023**, *38*, 2195832.

Xu, S.; Xiao, W.; Yu, C.; Chen, H.; Tan, Y. Mapping Cropland Abandonment in Mountainous Areas in China Using the Google Earth Engine Platform. *Remote Sens.* **2023**, *15*, 1145.

Yu, Z.; Di, L.; Rahman, M.S.; Tang, J. (2020). Fishpond Mapping by Spectral and Spatial Based Filtering on Google Earth Engine: A Case Study in Singra Upazila of Bangladesh. Remote Sens. 2020, 12, 2692. https://doi.org/10.3390/rs12

Zanaga, D.; van de Kerchove, R.; de Keersmaecker, W.; Souverijns, N.; Brockmann, C.; Quast, R.; Wevers, J.; Grosu, A.; Paccini, A.; Vergnaud, S.; *et al.* ESA WorldCover 10 m 2020 v100. 2021. Available online: **https://worldcover2020.esa.int/download** (accessed on 15 July 2024).

Zhang, P.; Hu, S.; Li, W.; Zhang, C. Parcel-level mapping of crops in a smallholder agricultural area: A case of central China using single-temporal VHSR imagery. *Comput. Electron. Agric.* **2020**, *175*, 105581.